Non-Pratt component of oceanic isostasy

James A. Conder*
DEPARTMENT OF GEOLOGY, SOUTHERN ILLINOIS UNIVERSITY, CARBONDALE, ILLINOIS 62901, USA

ABSTRACT

Oceanic lithosphere is understood to cool and subside away from mid-ocean ridges to a Pratt-like isostasy condition. However, the presence of ocean mass added on top of subsiding lithosphere necessitates an additional isostatic response that cannot be achieved through a Pratt model. In a manner similar to an ice cap on a continent, the addition of ocean mass on top of subsiding lithosphere drives a small degree of flow in the asthenosphere to accommodate the excess mass accumulated on top. The basic mathematics behind the isostasy-driven asthenospheric flow demonstrate that the flow occurs systematically from beneath younger seafloor toward older seafloor. The flow rate peaks beneath seafloor of about one-quarter the plate age. The maximum flow rate is a few tenths of a percent of the plate rate and is superimposed on the regional asthenospheric flow field. The modification to the regional flow induces a small, but systematically positive drag (mantle push) component on the overlying lithosphere. The form of the drag predisposes young lithosphere to extensional stress and older lithosphere to compressional stress.

LITHOSPHERE; v. 4; no. 5; p. 430–434 | Published online 5 September 2012 doi: 10.1130/L229.1

INTRODUCTION

Isostasy governs the first-order topography of the planet. The principle of isostasy states that adjacent columns of mass will be balanced in pressure at some compensation depth. So, to be in isostatic equilibrium, any mass excess at the surface (such as a mountain range) must be compensated by a mass deficit below the surface and vice versa, so that the pressures at the compensation depth from the overlying masses are constant for each column. Pratt and Airy isostasy, two well-known isostatic models, account for mass excesses in different ways. The Airy model compensates an excess mass at the surface with a low-density root extending into a higher-density substrate (Fig. 1A). The Pratt model compensates by having different-density columns of different heights (Fig. 1B). The well-known square root of the time subsidence curve for the seafloor is widely accepted as a Pratt response (Lowrie, 2007). As the seafloor is rafted away from the thin lithosphere at a mid-ocean-ridge spreading center, conductive cooling of the lithosphere from the top down makes it denser, systematically deepening and thickening lithosphere away from the axis. The conductive cooling in time leads to the well-established square root of the age subsidence curve (Parsons and Sclater, 1977; Stein and Stein, 1992).

The standard equation for analyzing seafloor subsidence due to conductive cooling is:

$$d = d_0 + c\sqrt{t}, \quad (1)$$

where d is ocean depth, d_0 is ridge depth, and t is seafloor age. The subsidence constant, c, depends on thermal expansion, α, mantle temperature, T_m, thermal diffusivity, κ, mantle density, ρ_m at temperature T_m, and ocean density, ρ_w,

$$c = 2\alpha T_m \sqrt{\kappa/\pi}\rho_m/(\rho_m - \rho_w), \quad (2)$$

(Lago et al., 1990). The last factor, $\rho_m/(\rho_m - \rho_w)$, accounts for the added mass to columns due to the overlying ocean. Subaerially, this factor goes to unity, and the subsidence curve reflects only cooling of the lithosphere.

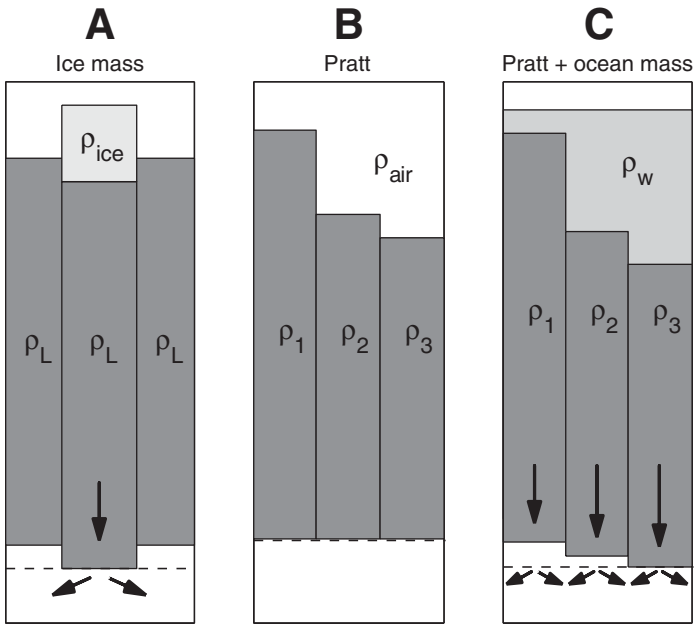

Figure 1. Isostasy models. Dashed lines denote compensation depths. (A) Airy isostasy for an ice cap overlying a constant-density, constant-thickness crust. The base of the crust is deflected downward as a low-density root to balance the excess mass of the ice sheet at top. The downward deflection requires displacement of underlying asthenosphere (arrows). (B) Pratt isostasy. Columns of different density are balanced at compensation depth. Subaerial cooling of spreading would follow a solely Pratt condition. (C) Pratt isostasy plus oceanic loading. For cooling in the oceans, Pratt isostasy is primary, but the input from the ocean is an added effect acting like the ice cap in A, where the entire column is deflected downward and must displace some underlying asthenosphere. Because the seafloor is expanding, the compensation depth is also increasing. The direction of displacement depends on the relative subsidence rates of the columns.

*E-mail: conder@geo.siu.edu.

Seafloor subsidence increases by adding more mass (ocean thickness) to deeper seafloor. For mantle density of 3330 kg/m^3 and seawater density of 1030 kg/m^3, this implies a submarine subsidence constant ~45% larger than a subaerial subsidence constant (Fig. 2).

This formulation has been used in a wide number of studies to examine different planetary processes (e.g., Crosby et al., 2006; Korenaga and Korenaga, 2008; Perrot et al., 1998; Wei and Sandwell, 2006). Invariably, this formulation is treated as a static condition, as one would expect for a sole Pratt response to seafloor cooling. Hofmeister and Criss (2006) pointed out that there is a conservation of rock mass problem in the formulation that arises with the inclusion of the overlying ocean. In short, adding an ocean is much like adding an ice cap. The additional mass in the previously equilibrated column is now out of equilibrium with its neighbors, and there is no degree of vertical depression and associated compression that can accommodate the inequality. Further depression would simply lead to more mass added to the column as more ocean fills in the void. So, in the presence of any overlying fluid with non-negligible mass, the downward deflection from lithospheric cooling by itself cannot lead to fully equilibrated Pratt isostasy and must have an Airy-like component.

The free-air gravity anomaly for compensated topography tends to zero. Across a 100 m.y. isostatically compensated oceanic plate, the total expected variation in free-air anomaly is 15–20 mGal, mimicking the seafloor depth curve (Crosby et al., 2006). Observed and predicted free-air anomalies for the oceans are shown in Figure 2B. The predicted free-air anomalies are for seafloor with subsidence rates predicted by Equations 1 and 2, including the overlying sea water while conserving mass in lithospheric columns. Anomalies are calculated by discretizing the excess masses into horizontal prisms and summing their vertical gravity attractions using the *gbox* algorithm (Blakely, 1996). For sole Pratt subsidence, the uncompensated portion of the lithosphere deepens and thickens with time, predicting larger free-air gravity anomalies over older oceanic lithosphere, comprising a total variation across the plate of more than 80 mGal. The observed anomalies for much of the oceans are small and tend to follow the depth-age curve (interrupted by seamounts) over much of their extent (Sandwell and Smith, 2009) (Fig. 2B), demonstrating isostatically compensated lithosphere in the oceans.

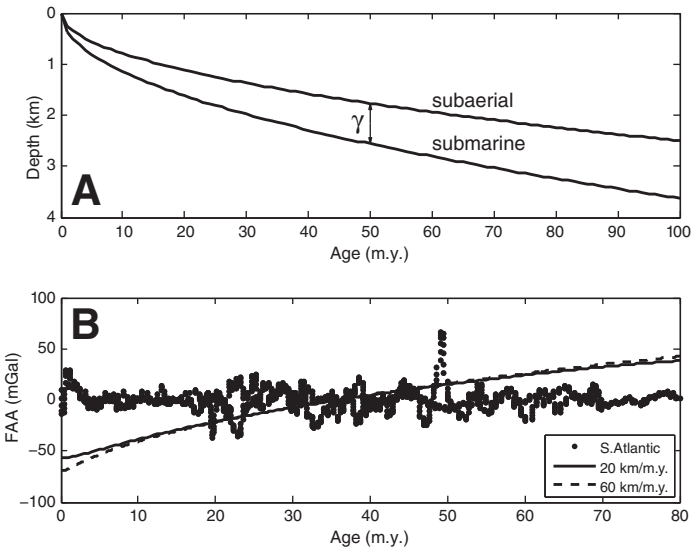

Figure 2. (A) Subaerial and submarine subsidence curves following Equations 1 and 2. The difference, γ, is the height of asthenosphere column that is equivalent to the mass of the overlying ocean. (B) Free-air gravity anomalies (FAA). Dots are observed anomalies from ERS-1 (Sandwell and Smith, 2009) with ages from Müller et al. (2008). Two representative profiles from the South Atlantic are presented: One along 10°S and one from 20°S, with both extending from 35°W to 0°E. Solid and dashed lines show the expected free-air gravity anomaly for a seafloor subsiding according to Equations 1 and 2, with no redistribution of mass in the asthenosphere as response to the subsidence. The predicted free-air gravity anomaly depends only weakly on spreading rate.

The conundrum of the impossibility of fully Pratt-compensated seafloor in the presence of equilibrated lithosphere is straightforwardly reconciled by recognizing rock mass redistribution among columns. For oceanic isostasy, this transfer can be accomplished directly through asthenosphere flow, just as isostatically compensated ice-capped continents require displacement of asthenosphere to achieve equilibrium (Fig. 1). In other words, depression of the surface to deepen the root must come with the removal of some higher-density material from that column (through asthenosphere displacement), without which the extra mass in that column can never be equilibrated with other lithospheric columns having different ocean depths. Figure 1C shows the increasing depth to the base of the depressed gray boxes. The depth to the deepest base is the compensation depth. Importantly, the column heights of the "unaffected mantle" below the gray boxes are now variable. The equilibration flow must occur within this mantle beneath the gray boxes. Equations 1 and 2 implicitly capture this dynamic, despite being typically viewed and treated as a static isostasy condition.

Here, I explore the first-order isostatic dynamic response of the asthenosphere arising from lithospheric isostasy in the presence of an ocean. In this vein, I lay out the basic mathematical underpinnings of the dynamics. The primary result is a sustained asthenosphere flow from beneath young seafloor to beneath old seafloor that arises with isostatic adjustment to continual spreading and seafloor deepening.

MATHEMATICAL DEVELOPMENT

The difference between the subaerial and submarine depth-age curves reflects the integrated amount of mass displaced from any given mass column. The amount of mass that must be removed from any column is equal to a column of the same dimension as additional subsidence arising from the overlying ocean. So, the relevant curve to explore this redistribution is

$$\gamma = c^* \sqrt{t}, \tag{3}$$

where γ is the difference between subaerial and submarine subsidence curves, and

$$c^* = c_{submarine} - c_{subaerial}. \tag{4}$$

Values for $c_{submarine}$ and $c_{subaerial}$ may be deduced by plugging in reasonable values for all the parameters in Equation 2. Here, I use "typical" values (Turcotte and Schubert, 2002), $\alpha = 3 \times 10^{-5}$ K^{-1} and $\kappa = 30$ km^2/m.y., $T_m = 1350$ °C, $\rho_m = 3330$ kg/m^3, and $\rho_w = 1030$ kg/m^3. Laboratory experiments suggest that α for forsterite at temperatures and pressures important for plate cooling is in the range of 4–5 × 10^{-5} K^{-1} (Katsura et al., 2009). However, values in this range substantially overpredict subsidence. The difference may be a result of finite rigidity in the shallow lithosphere (Korenaga and Korenaga, 2008). In any case, the effective thermal expansivity is the relevant parameter here, resulting in a $c^* = 0.11$ km/m.y.$^{1/2}$

Because the system is constantly adjusting to account for the excess, the more useful parameter to examine is the rate of excess increase. To get the rate of mass excess accumulation in each column, one can differentiate Equation 3 with respect to time,

$$\dot{\gamma} = \frac{c^*}{2\sqrt{t}}. \tag{5}$$

So, the rate of mass increase for all columns, Γ, in a subsiding ocean basin profile with plate velocity v and oldest seafloor, t_A, is

$$\Gamma = \frac{c^* v}{2}\int_0^{t_A}\frac{1}{\sqrt{t}}dt, \quad (6)$$

or

$$\Gamma = c^* v\sqrt{t_A}. \quad (7)$$

The accommodation need only redistribute the fraction of the accumulated mass that is in isostatic disequilibrium, i.e., not all mass that is gained across columns is out of isostatic equilibrium. Thus, it is the differences in mass accumulation across the columns that contribute to the isostatic excesses.

Because younger seafloor subsides more rapidly than older seafloor, isostatic excess is added more rapidly beneath young seafloor than beneath older seafloor (Fig. 3A). For the system to constantly re-equilibrate, asthenosphere must be redistributed toward older seafloor (Fig. 3B) requiring a degree of asthenospheric flow away from ridge axes. Because lithosphere is thicker away from ridge axes, it is somewhat counterintuitive from Figure 1C that flow would be toward older seafloor. However, most of the thickening undergone by older lithosphere took place at younger ages and has already been accommodated. Thus, it is the current lithosphere thickening rate that drives the flow.

The crossover age, t_c, denotes the age of the column with a mass accumulation rate equal to the mean accumulation rate across the plate. So,

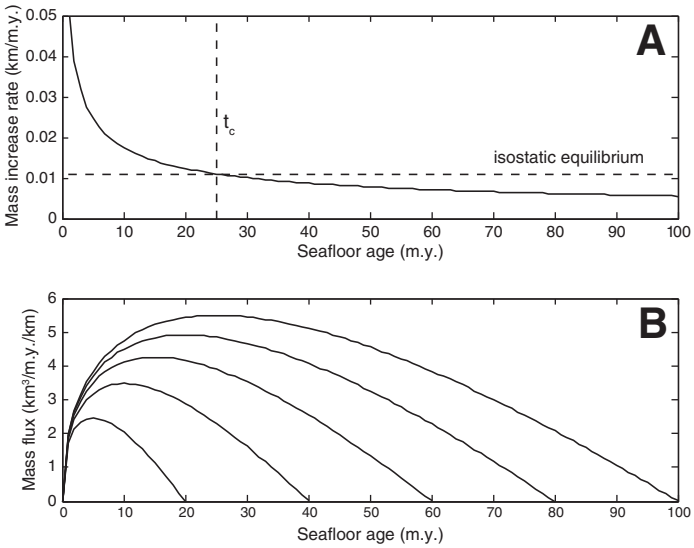

Figure 3. (A) The isostatic excess growth rate. The total mass increase rates for columns of given age are shown as the solid curve. The isostatic excesses are deviations of the solid curve to the horizontal dashed line. The vertical dashed line shows t_c, the age of the lithosphere where isostatic excess growth rate is zero. Without asthenospheric readjustment, isostatic excesses would build under young seafloor, and isostatic deficits would accumulate under old seafloor. (B) Mass flux of asthenosphere readjustment. To redistribute mass in the asthenosphere toward isostatic equilibrium, mass flux is from beneath young seafloor to beneath older seafloor. As all the excess must move across t_c, the mass flux is greatest there and decreases as mass is redistributed beneath older seafloor until the instantaneous mass flux reaches zero beneath the oldest seafloor. Because seafloor is growing with time, the mass flux is also evolving. The five curves shown denote the instantaneous mass fluxes (Eq. 13) for oceanic plates of 20, 40, 60, 80, and 100 m.y. ages.

$$\frac{c^*}{2\sqrt{t_c}} = \frac{\Gamma}{vt_A}, \quad (8)$$

which leads to

$$t_c = t_A/4. \quad (9)$$

This crossover age is convenient to quantitatively examine the way in which material must be redistributed within the asthenosphere (Fig. 3). By comparing the fraction of Γ between 0 and t_c with that between t_c and t_A, and noting that all columns must tend to the mean to achieve equilibrium, it can be shown that the total material that must be redistributed from beneath young seafloor to beneath older seafloor is Γ/4. That is, a volume of Γ/4 asthenosphere must be physically transferred across the seafloor of age t_c. For seafloor like the northern Atlantic, with velocity of 20 km/m.y. and 100-m.y.-old crust, roughly 20 km³/m.y. of asthenosphere per kilometer of ridge length must be accommodated across the basin by physically moving 5 km³ of asthenosphere from beneath seafloor younger than 25 m.y. to beneath seafloor older than 25 m.y. A faster and older plate, like the Pacific, will have correspondingly more asthenosphere material to transfer.

To maintain isostatic equilibrium in the oceans, mass balance dictates that lateral asthenosphere flow must balance the isostatic excesses (positive and negative) from subsidence. The change in mass in a column due to lateral asthenosphere flow is simply the mass flux into the column minus the mass flux out of the column. For one-dimensional flow, the governing equation is

$$\dot{\gamma}^* - \frac{dU}{dx} = 0, \quad (10)$$

where $\dot{\gamma}^*$ is the isostatic excess accumulation during subsidence,

$$\dot{\gamma}^* = \dot{\gamma} - \frac{c^*}{2\sqrt{t_c}}, \quad (11)$$

and U is the lateral asthenosphere mass flux (in units of km²/m.y.). Therefore, $\dot{\gamma}^*$ is positive for seafloor younger than t_c and negative for seafloor older than t_c. The flux as a function of position, $U(x)$, may be determined by

$$U(x) = \int_0^x \frac{dU}{dx}dx, \quad (12)$$

leading to

$$U(x) = c^*\sqrt{v}\left(\sqrt{x} - \frac{x}{2\sqrt{x_c}}\right), \quad (13)$$

with $x = vt$ and $x_c = vt_c$.

Beneath young seafloor, mass must be wicked away to balance the increasing isostatic excess, so dU/dx is positive. Likewise, mass must be added beneath older seafloor to balance the isostatic deficit, requiring negative dU/dx. At t_c, zero net mass is to be added or removed, requiring that $dU/dx = 0$. This requirement means that the maximum flux is beneath seafloor of age t_c (Fig. 3). Equation 13 is for the instantaneous flux. However, because the seafloor is continually spreading, t_A and t_c are also increasing with time. The evolution of the mass flux function is shown in Figure 3B. The mass flux is zero at the ridge, increases rapidly toward a maximum lateral flux at t_c, and then decreases to zero at t_A. As t_A increases, the maximum shifts toward older ages, and overall magnitude increases to accommodate the larger volume of isostatic excesses to be accommodated for the increasing width of seafloor (Fig. 3B).

The total flux, Υ_m, of transferred material can be determined by integrating $U(x)$ over the width of the plate,

$$\Upsilon_m = \frac{1}{6} c * v^2 t_A^{3/2}. \quad (14)$$

The units of the total flux Υ_m are km^3/m.y. Υ_m is proportional to v^2 because both the distance required for redistribution and Γ at time t_A scale with v. Of course, no one parcel needs to travel the full distance, as a larger volume of asthenosphere may be mobilized to achieve isostatic equilibrium. However, the integral of the full volume of mobilized asthenosphere per ridge length multiplied by the horizontal distance over which each mobilized parcel is displaced must equal Υ_m.

DISCUSSION

The flow rate in the asthenosphere depends on the thickness of the asthenospheric channel accommodating the flow. For simple Poiselle flow in a homogeneous layer of thickness H, the excess flow, u, will follow the form

$$u = 1.5 u_{ave} \left(1 - \frac{z^2}{H^2}\right), \quad (15)$$

where u_{ave} is defined by U/H, and z equals zero at the channel midpoint. Assuming mobilization throughout a 100-km-thick asthenosphere channel, the flow peaks at a few tenths of a percent of the plate spreading rate.

Although the flow rate induced by isostatic equilibrium is only a small fraction of the spreading rate, the flow is systematically positive in the plate spreading direction. It has long been noted that plates moving over a static mantle should experience a resistive drag (e.g., Forsyth and Uyeda, 1975). The necessary component of flow in the asthenosphere in the same direction as the plate spreading direction from constant isostatic adjustment serves to systematically reduce resistive tractions and increase driving tractions. The magnitude of the shear traction at the base of the lithosphere may be determined by differentiating Equation 15 with respect to z at $H/2$ and multiplying by viscosity. For a viscosity of 5×10^{19} Pa s, the basal traction is found to be 2400 N per meter of ridge length at x_c. Integrating over a 2000-km-wide plate, the traction is ~5×10^9 N/m in the positive direction. This magnitude is small compared to other driving forces, such as ridge push or slab pull, on the order of 10^{12}–10^{13} N/m (Turcotte and Schubert, 2002), but it is also always in the driving direction.

Globally, possibly ~50% of the magnitude of Earth's deviatoric stress field arises from lithosphere-asthenosphere tractions (Ghosh et al., 2008). Regional asthenosphere flow can act as an important tectonic driver and influence other aspects of lithospheric evolution. For instance, Barba et al. (2008) showed that a strong mantle flow is required to explain stress indicators on the Italian peninsula. Likewise, a strong, regional asthenospheric flow likely develops around the Pacific Superswell, leading to asymmetric subsidence and seismic signatures along the southern East Pacific Rise (Conder et al., 2002; Conder, 2007; Toomey et al., 2002). Other regions of asymmetric subsidence (Marty and Cazenave, 1989; Phipps Morgan and Smith, 1992) are likely regions of regionally important asthenospheric flow, as is the mantle wedge of some subduction zones (Conder and Wiens, 2007; Kneller and van Keken, 2007; Pozgay et al., 2007). Isostasy-driven flow is clearly small in comparison to regional variations, but because it is pervasive and additive to other induced flows, it could have significance on platewide and global scales.

The flow may have a more substantive effect on stresses in the plate interior. Because the flow rate changes across the plate (Fig. 3B), younger portions of oceanic plates will tend to be put into tension, and older portions of the plate will tend to be put into compression. Figure 4 shows non–plate-boundary–related observations for the oceans from the World Stress Map (Heidbach et al., 2010). While somewhat sparse, histograms of the distributions of extensional and compressive observations with relation to seafloor age normalized by plate age are noticeably dissimilar (Fig. 4B). A Kolmogorov-Smirnov two-sample test verifies that the two populations are distinct at well above 99.9% confidence. The largest number of both occurs on seafloor of less than one-quarter plate age, where the bulk of the observations lie. However, extensional stresses dominate over compressional stresses (Fig. 4C). On older seafloor, the opposite is true. Although it is not necessarily the case that isostatic flow is the cause behind any particular observation, it is reasonable to infer that, in general, isostatic flow biases older seafloor toward compression and younger seafloor toward extension.

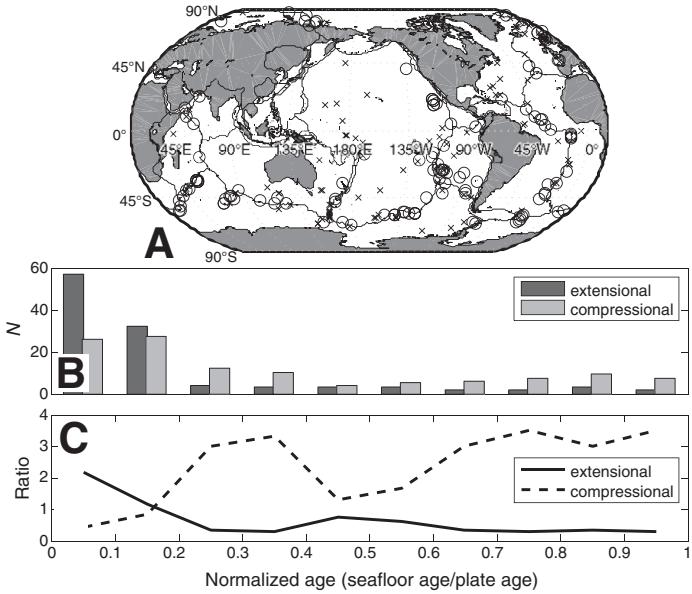

Figure 4. Oceanic intraplate stress observations from World Stress Map (WSM, 2012). Only data tagged as unassociated with plate-boundary activity by WSM are used. Data likely associated with other identifiable tectonic processes (outer rises, hotspots, microplates, and diffuse boundaries) as well as those on the seafloor not associated with active crustal accretion are excluded, leaving 127 extensional and 134 compressional data points remaining for analysis. (A) WSM observations used in B and C. Open circles denote extensional stress observations, and crosses denote compressional observations. Ages are from Müller et al. (2008). Plate ages for each observation are found by following seafloor age gradient to termination. (B) Histograms of extensional and compressional observations by normalized age. (C) Ratios of histograms showing dominance of extensional intraplate stresses at young ages and compressional stresses at older ages.

CONCLUSIONS

Isostasy in the oceans has traditionally been viewed as a static Pratt process. However, in the presence of an overlying ocean, subsidence due to cooling drives a dynamic response in the asthenosphere below. Isostatically driven flow in the asthenosphere is everywhere directed from beneath young seafloor to beneath older seafloor. This dynamic response is necessary to achieve isostatic equilibrium for oceanic lithosphere and accounts for roughly one-third of seafloor isostatic accommodation. The flow rate is a few orders of magnitude smaller than, but proportional to, the plate spreading rate. This flow, directed from beneath young seafloor toward older seafloor, imparts a lithosphere basal traction systematically in the positive direction. The flow peaks beneath seafloor of about one-quarter the plate age, potentially biasing younger seafloor to extensional intraplate stress and older seafloor to compressional intraplate stress.

ACKNOWLEDGMENTS

I thank Don Forsyth, Andrew Dombard, and Clint Conrad for insightful comments and discussions regarding oceanic isostasy and flow in the asthenosphere. Comments from an anonymous reviewer improved the paper. This work was partially supported by National Science Foundation grant OCE-0426408.

REFERENCES CITED

Barba, S., Carafa, M.M.C., and Boschi, E., 2008, Experimental evidence for mantle drag in the Mediterranean: Geophysical Research Letters, v. 35, no. 6, p. 1–6, doi:10.1029/2008GL033281.

Blakely, R.J., 1996, Potential Theory in Gravity and Magnetic Applications: New York, Cambridge University Press, 441 p.

Conder, J.A., 2007, Dynamically driven mantle flow and shear wave splitting asymmetry across the EPR, MELT area: Geophysical Research Letters, v. 34, no. 16, p. 1–5, doi:10.1029/2007GL030832.

Conder, J.A., and Wiens, D.A., 2007, Rapid mantle flow beneath the Tonga volcanic arc: Earth and Planetary Science Letters, v. 264, no. 1–2, p. 299–307, doi:10.1016/j.epsl.2007.10.014.

Conder, J.A., Forsyth, D.W., and Parmentier, E.M., 2002, Asthenospheric flow and asymmetry of the East Pacific Rise, MELT area: Journal of Geophysical Research, v. 107, no. B12, doi:10.1029/2001JB000807.

Crosby, A.G., McKenzie, D., and Sclater, J.G., 2006, The relationship between depth, age and gravity in the oceans: Geophysical Journal International, v. 166, no. 2, p. 553–573, doi:10.1111/j.1365-246X.2006.03015.x.

Forsyth, D., and Uyeda, S., 1975, On the relative importance of the driving forces of plate motion: Geophysical Journal International, v. 43, no. 1, p. 163–200, doi:10.1111/j.1365-246X.1975.tb00631.x.

Ghosh, A., Holt, W.E., Wen, L., Haines, A.J., and Flesch, L.M., 2008, Joint modeling of lithosphere and mantle dynamics elucidating lithosphere-mantle coupling: Geophysical Research Letters, v. 35, no. 16, p. 1–5, doi:10.1029/2008GL034365.

Heidbach, O., Tingay, M., Barth, A., Reinecker, J., Kurfeß, D., and Müller, B., 2010, Global crustal stress pattern based on the World Stress Map database release 2008: Tectonophysics, v. 482, no. 1–4, p. 3–15, doi:10.1016/j.tecto.2009.07.023.

Hofmeister, A.M., and Criss, R.E., 2006, Comment on "Estimates of heat flow from Cenozoic seafloor using global depth and age data," by M. Wei and D. Sandwell: Tectonophysics, v. 428, no. 1–4, p. 95–100, doi: 10.1016/j.tecto.2006.08.010.

Katsura, T., Shatskiy, A., Manthilake, M.A.G.M., Zhai, S., Fukui, H., Yamazaki, D., Matsuzaki, T., Yoneda, A., Ito, E., Kuwata, A., Ueda, A., Nozawa, A., and Funakoshi, K.-i., 2009, Thermal expansion of forsterite at high pressures determined by in situ X-ray diffraction: The adiabatic geotherm in the upper mantle: Physics of the Earth and Planetary Interiors, v. 174, no. 1–4, p. 86–92, doi:10.1016/j.pepi.2008.08.002.

Kneller, E.A., and van Keken, P.E., 2007, Trench-parallel flow and seismic anisotropy in the Mariana and Andean subduction systems: Nature, v. 450, no. 7173, p. 1222–1225, doi:10.1038/nature06429.

Korenaga, T., and Korenaga, J., 2008, Subsidence of normal oceanic lithosphere, apparent thermal expansivity, and seafloor flattening: Earth and Planetary Science Letters, v. 268, no. 1–2, p. 41–51, doi:10.1016/j.epsl.2007.12.022.

Lago, B., Cazenave, A., and Marty, J.-C., 1990, Regional variations in subsidence rate of lithospheric plates: Implication for thermal cooling models: Physics of the Earth and Planetary Interiors, v. 61, no. 3–4, p. 253–259, doi:10.1016/0031-9201(90)90109-B.

Lowrie, W., 2007, Fundamentals of Geophysics, 2nd Edition: New York, Cambridge University Press, 381 p.

Marty, J.C., and Cazenave, A., 1989, Regional variations in subsidence rate of oceanic plates: A global analysis: Earth and Planetary Science Letters, v. 94, no. 3–4, p. 301–315, doi:10.1016/0012-821X(89)90148-9.

Müller, R.D., Sdrolias, M., Gaina, C., and Roest, W.R., 2008, Age, spreading rates, and spreading asymmetry of the world's ocean crust: Geochemistry, Geophysics, Geosystems, v. 9, no. 4, p. 1–19, doi:10.1029/2007GC001743.

Parsons, B., and Sclater, J.G., 1977, An analysis of the variation of ocean floor bathymetry and heat flow with age: Journal of Geophysical Research, v. 82, no. 5, p. 803–827, doi:10.1029/JB082i005p00803.

Perrot, K., Francheteau, J., Maia, M., and Tisseau, C., 1998, Spatial and temporal variations of subsidence of the East Pacific Rise (0–23°S): Earth and Planetary Science Letters, v. 160, no. 3–4, p. 593–607, doi:10.1016/S0012-821X(98)00114-9.

Phipps Morgan, J., and Smith, W.H.F., 1992, Flattening of the sea-floor depth-age curve as a response to asthenospheric flow: Nature, v. 359, no. 6395, p. 524–527, doi:10.1038/359524a0.

Pozgay, S.H., Wiens, D.A., Conder, J.A., Shiobara, H., and Sugioka, H., 2007, Complex mantle flow in the Mariana subduction system: Evidence from shear wave splitting: Geophysical Journal International, v. 170, no. 1, p. 371–386, doi:10.1111/j.1365-246X.2007.03433.x.

Sandwell, D.T., and Smith, W.H.F., 2009, Global marine gravity from retracked Geosat and ERS-1 altimetry: Ridge segmentation versus spreading rate: Journal of Geophysical Research, v. 114, no. B1, p. 1–18, doi:10.1029/2008JB006008.

Stein, C.A., and Stein, S., 1992, A model for the global variation in oceanic depth and heat flow with lithospheric age: Nature, v. 359, no. 6391, p. 123–129, doi:10.1038/359123a0.

Toomey, D.R., Wilcock, W.S.D., Conder, J.A., Forsyth, D.W., Blundy, J.D., Parmentier, E.M., and Hammond, W.C., 2002, Asymmetric mantle dynamics in the MELT region of the East Pacific Rise: Earth and Planetary Science Letters, v. 200, no. 3–4, p. 287–295, doi:10.1016/S0012-821X(02)00655-6.

Turcotte, D.L., and Schubert, G., 2002, Geodynamics, 2nd Edition: New York, Cambridge University Press, 456 p.

Wei, M., and Sandwell, D., 2006, Estimates of heat flow from Cenozoic seafloor using global depth and age data: Tectonophysics, v. 417, no. 3–4, p. 325–335, doi:10.1016/j.tecto.2006.02.004.

World Stress Map (WSM), 2012, World Stress Map: http://worldstressmap.org (accessed 23 May 2012).

MANUSCRIPT RECEIVED 29 MAY 2012
REVISED MANUSCRIPT RECEIVED 24 JUNE 2012
MANUSCRIPT ACCEPTED 6 JULY 2012

PRINTED IN THE USA